

## Regimes of chemical reaction waves initiated by nonuniform initial conditions for detailed chemical reaction models

M. A. Liberman,<sup>1,2,\*</sup> A. D. Kiverin,<sup>3</sup> and M. F. Ivanov<sup>3</sup>

<sup>1</sup>*Skobel'syn Institute of Nuclear Physics, Moscow State University, 119991 Moscow, Russia*

<sup>2</sup>*Department of Physics and Astronomy, Uppsala University, Box 530, SE-751 21, Uppsala Sweden*

<sup>3</sup>*Joint Institute for High Temperatures, Russian Academy of Science, Izhorskaya 13, Building 2 Moscow 125412, Russia*

(Received 27 February 2012; revised manuscript received 24 April 2012; published 25 May 2012)

Regimes of chemical reaction wave propagation initiated by initial temperature nonuniformity in gaseous mixtures, whose chemistry is governed by chain-branching kinetics, are studied using a multispecies transport model and a detailed chemical model. Possible regimes of reaction wave propagation are identified for stoichiometric hydrogen-oxygen and hydrogen-air mixtures in a wide range of initial pressures and temperature levels, depending on the initial non-uniformity steepness. The limits of the regimes of reaction wave propagation depend upon the values of the spontaneous wave speed and the characteristic velocities of the problem. It is shown that one-step kinetics cannot reproduce either quantitative neither qualitative features of the ignition process in real gaseous mixtures because the difference between the induction time and the time when the exothermic reaction begins significantly affects the ignition, evolution, and coupling of the spontaneous reaction wave and the pressure wave, especially at lower temperatures. We show that all the regimes initiated by the temperature gradient occur for much shallower temperature gradients than predicted by a one-step model. The difference is very large for lower initial pressures and for slowly reacting mixtures. In this way the paper provides an answer to questions, important in practice, about the ignition energy, its distribution, and the scale of the initial nonuniformity required for ignition in one or another regime of combustion wave propagation.

DOI: [10.1103/PhysRevE.85.056312](https://doi.org/10.1103/PhysRevE.85.056312)

PACS number(s): 47.70.Pq, 82.33.Vx, 47.40.Rs

### I. INTRODUCTION

The initiation or ignition of a chemical reaction is one of the most important and fundamental problems in combustion physics. One needs to know how combustion starts and how the initial conditions influence the regime of the reaction wave which propagates out from the ignition location. What type of combustion wave is formed, depending on the ignition conditions? The ignition problem is also important for improving combustion safety and understanding ignition risk assessments of processes where hydrocarbons are oxidized at different initial conditions of concentration, temperature and pressure. How can we minimize “accidental” explosions in mines, and nuclear power plants? An important problem of “hydrogen safety” is connected with leakage of the hydrogen and its further explosion.

In most practical cases ignition arises from a small area of combustible mixture which is locally heated by means of an electric spark, hot wire, focused laser light, and the like. Such local energy release results in the formation of an initial nonuniform distribution of temperature (in the general case, the temperature and concentration of reagents), which determines the further evolution of the reaction wave depending on the mixture reactivity and the initial pressure. Examples of such initial nonuniform distributions of temperature and concentration are the energy deposition from a spark plug in an engine combustor [1] or hydrogen gas leakage and its nonuniform distribution by convective flow in a room. In both cases the initial nonuniform distribution of temperature and concentration may result in ignition (thermal explosion).

The ignition and possible regimes of a propagating chemical reaction wave ignited by the initial temperature gradient were studied for the first time by Zeldovich [2], using a one-step chemical reaction model. The basic idea of the Zeldovich description was that a spontaneous reaction wave can propagate through a reactive material along a spatial gradient of temperature [ $\nabla T(x)$ ] or any other value which influences the reaction ignition time (the induction time). For a one-step chemical model the induction time is defined by the time scale of the maximum reaction rate. In the case of real chain-branching chemistry this is the time scale for the stage of endothermic chain initiation and branching reactions. This quantity is measured experimentally and determines local properties of the combustible mixture depending on its thermodynamic state. The reaction begins at the point of minimum induction time  $\tau_{\text{ind}}(T(x))$  and correspondingly maximum temperature and spreads along the gradient by spontaneous ignition at neighboring locations where  $\tau_{\text{ind}}$  is longer. The spontaneous reactive wave propagates in the direction of the temperature gradient with velocity

$$U_{\text{sp}} = |(d\tau_{\text{ind}}/dx)|^{-1} = |(\partial\tau_{\text{ind}}/\partial T)^{-1}(\partial T/\partial x)^{-1}|. \quad (1)$$

In general, there is no causal link between successive autoignitions and there is no restriction on the value of  $U_{\text{sp}}$ , which depends only on the gradient steepness and does not depend on thermal conduction or sound speed. In Ref. [3] Zeldovich and co-workers have shown that a shallow initial temperature gradient can ignite a detonation regime of combustion. In subsequent studies [4–10] researchers have employed a one-step Arrhenius reaction model and have been almost fully focused on the regime of direct ignition of a detonation by the initial temperature gradient. It should be noted, however, that the Zeldovich concept [2] of a

\*Corresponding author: [misha.liberman@gmail.com](mailto:misha.liberman@gmail.com), [mliberman@mics.msu.su](mailto:mliberman@mics.msu.su)

spontaneous reaction is much more valuable, because it opens an avenue to study the reaction ignition and different regimes of the reaction wave propagation initiated by the nonuniformity in temperature or reactivity caused by the initial local energy release, and is therefore of great fundamental and practical importance.

It became obvious in further studies [11–14] using simplified two-step and three-step models, which to some extent mimic the chain-branching kinetics with a simplified notional reaction scheme between a set of pseudospecies, that the one-step chemical model does not properly describe systems governed by chain-branching reactions. In particular, the role of the chain-branching crossover temperature in shock-induced ignition was studied by numerical simulation [14], and it was found that the results obtained using two-step and three-step models are qualitatively different from those obtained from a one-step model. It is anyway clear that these simplified chemical and gas-dynamics models may lead only to a general qualitative conclusion that the one-step model is not appropriate for simulating detonation initiation in systems governed by chain-branching reactions. However, the quantitative difference, important in practice, between a one-step model and realistic detailed chemical models remained unclear. All the same, it is known [15] that, for example, the ignition energy for a methane-air mixture computed using a one-step model differs by two orders of magnitude from the experimentally measured value. Results of earlier numerical studies [16] which used a detailed chemical kinetics model have shown that the steepness of the temperature gradient required for a direct detonation initiation is significantly smaller than that obtained for the same conditions for a one-step model. It should be stressed that although the previous studies have been almost solely focused on the particular case of direct ignition of detonation, the problem in question is much more general. It answers the practically important question of what are the propagating regimes of combustion wave which can be initiated by initial nonuniform energy deposition.

It is clear that the models with fairly simplified gas dynamics and chemical kinetics, although of interest to reduce computational cost and often allowing analytical analysis, may lead to only a very basic picture of the reaction process, describing qualitatively only a few major properties of the phenomena in question with poor accuracy, if any. To understand quantitative effects one should use full gas dynamics with real transport and thermodynamic properties for multicomponent gaseous mixtures and detailed chemical kinetics models. Such a level of modeling allows a clear understanding of the feedback between gas dynamics and chemistry, which is the principal point when studying the unsteady process of ignition and cannot be determined using simplified gas-dynamical and chemical models. What matters is to obtain realistic quantitative numerical values which define the scale of the initial nonuniform distribution of temperature capable of initiating one or another mode of combustion wave.

The present paper presents results on classification of the propagation regimes of the chemical reaction waves initiated by initial temperature nonuniformity in gaseous mixtures in a wide range of initial pressures and temperature levels, depending on the steepness of the temperature gradient, using high-resolution numerical simulations of the

reactive Navier-Stokes equations, including a multispecies transport model, the effects of viscosity, thermal conduction, and molecular diffusion. We consider the problem in question, using a detailed chemical reaction mechanism for hydrogen-oxygen and hydrogen-air mixtures, which are the quintessential examples of chain-branching reactions whose chemical kinetics is well understood and whose detailed chemical kinetic models are well known and relatively simple.

## II. PROBLEM SETUP

We consider uniform initial conditions apart from a linear temperature gradient. The model of the linear temperature gradient is convenient for analysis and it has been widely used in previous studies [2–14]. The emphasis will be on quantitative and/or qualitative comparison and contrasting of the results of detailed modeling with those obtained using a one-step chemical model. The initial conditions at  $t = 0$ , prior to ignition, are constant pressure and zero velocity of the unburned mixture. At the left boundary at  $x = 0$  the conditions are for a solid reflecting wall, where  $u(0, t) = 0$  and the initial temperature  $T = T^*$ . Thus, the initial conditions are quiescent and uniform, except for a linear gradient in temperature (and hence density):

$$T(x, 0) = T^* - (T^* - T_0)(x/L), \quad 0 \leq x \leq L, \quad (2)$$

$$P(x, 0) = P_0, \quad u(x, 0) = 0. \quad (3)$$

The initial temperature gradient is characterized by the maximum temperature  $T(0, 0) = T^*$  at the top left edge, by the background mixture temperature  $T(x > L, 0) = T_0$  outside the gradient, and by the gradient steepness  $(T^* - T_0)/L$ . For a linear temperature gradient it is convenient to introduce the “gradient scale” ( $L$ ), which characterizes the gradient steepness for a fixed value of  $(T^* - T_0)$  and can be viewed as the size of the area where the initial temperature gradient was created by the energy input or the like.

The governing equations are the one-dimensional time-dependent, multispecies reactive Navier-Stokes equations including the effects of compressibility, molecular diffusion, thermal conduction, viscosity, and chemical kinetics with subsequent chain branching, production of radicals, and energy release:

$$\frac{\partial \rho}{\partial t} + \frac{\partial(\rho u)}{\partial x} = 0, \quad (4)$$

$$\frac{\partial Y_i}{\partial t} + u \frac{\partial Y_i}{\partial x} = \frac{1}{\rho} \frac{\partial}{\partial x} \left( \rho D_i \frac{\partial Y_i}{\partial x} \right) + \left( \frac{\partial Y_i}{\partial t} \right)_{\text{ch}}, \quad (5)$$

$$\rho \left( \frac{\partial u}{\partial t} + u \frac{\partial u}{\partial x} \right) = - \frac{\partial P}{\partial x} + \frac{\partial \sigma_{xx}}{\partial x}, \quad (6)$$

$$\rho \left( \frac{\partial E}{\partial t} + u \frac{\partial E}{\partial x} \right) = - \frac{\partial(Pu)}{\partial x} + \frac{\partial}{\partial x} (\sigma_{xx} u) + \frac{\partial}{\partial x} \left( \kappa(T) \frac{\partial T}{\partial x} \right) + \sum_k \frac{h_k}{m_k} \left[ \frac{\partial}{\partial x} \left( \rho D_k(T) \frac{\partial Y_k}{\partial x} \right) \right], \quad (7)$$

$$P = R_B T n = \left( \sum_i \frac{R_B}{m_i} Y_i \right) \rho T = \rho T \sum_i R_i Y_i, \quad (8)$$

$$\varepsilon = c_v T + \sum_k \frac{h_k \rho_k}{\rho} = c_v T + \sum_k h_k Y_k, \quad (9)$$

$$\sigma_{xx} = \frac{4}{3} \mu \left( \frac{\partial u}{\partial x} \right). \quad (10)$$

Here we use the standard notations:  $P$ ,  $\rho$ , and  $u$ , are the pressure, mass density, and flow velocity,  $Y_i = \rho_i/\rho$  the mass fractions of the species,  $E = \varepsilon + u^2/2$  the total energy density,  $\varepsilon$  the inner energy density,  $R_B$  the universal gas constant,  $m_i$  the molar mass of species  $i$ ,  $R_i = R_B/m_i$ ,  $n$  the molar density,  $\sigma_{ij}$  the viscous stress tensor,  $c_v = \sum_i c_{vi} Y_i$  the constant-volume specific heat,  $c_{vi}$  the constant-volume specific heat of species  $i$ ,  $h_i$  the enthalpy of formation of species  $i$ ,  $\kappa(T)$  and  $\mu(T)$  the coefficients of thermal conductivity and viscosity,  $D_i(T)$  the diffusion coefficients of species  $i$ , and  $(\partial Y_i/\partial t)_{\text{ch}}$  the variation of concentration (mass fraction) of species  $i$  in the chemical reactions.

The equations of state for the reactive mixture and for the combustion products were taken with the temperature dependence of the specific heats and enthalpies of each species from the Joint Army Navy NASA Air Force Thermochemical Tables (JANAF) and interpolated by fifth-order polynomials [17,18]. The viscosity and thermal conductivity coefficients of the mixture were calculated from the gas kinetic theory using the Lennard-Jones potential [19]. The coefficients of the heat conduction of the  $i$ th species  $\kappa_i = \mu_i c_{pi}/\text{Pr}$  are expressed via the viscosity  $\mu_i$  and the Prandtl number,  $\text{Pr} = 0.75$ .

The numerical method is based on splitting of the Eulerian and Lagrangian stages, known as the coarse particle method (CPM) [20]. A detailed description of the modified CPM, optimal approximation scheme, details of the equations and transport coefficients, and the reaction kinetics scheme together with the reaction rates were published in Refs. [21,22]. The reaction kinetics scheme has been thoroughly tested and successfully used in many practical applications [23,24].

The convergence of the solutions and proper resolution are of paramount importance to verify that the observed phenomena are sufficiently resolved, especially when computational fluid dynamics (CFD) simulations are used with a detailed chemical reaction model. The convergence and resolution tests outlined in the Appendix have shown that a resolution of 50 computational cells over the width of the laminar flame (for example,  $\Delta = 0.0064$  mm at  $P_0 = 1$  atm and much smaller for higher pressure) provides a good convergence and captures correctly the details of the observed processes.

### III. DETAILED CHEMISTRY AND ONE-STEP MODEL INDUCTION TIMES

The chain-branching  $\text{H}_2\text{-O}_2$  reaction begins with the induction stage of radical formation followed by the main stage of the exothermic reactions of chain termination [25,26]. There are two fundamental differences between the chain-branching reactions and a single-step model. First, the induction time for a single-step Arrhenius model is several orders of magnitude shorter than the induction time for the real chemical schemes, especially in the range of ignition temperatures  $T < 1200$  K (see, e.g. Figs. 1 and 2 in Ref. [21] where a single-step model was fitted using the laminar normal flame velocity value). When using a one-step model one has to make a choice of how

to fit the model parameters, which depends on the application. For a stationary problem, e.g., for a stationary planar flame, one can choose the model parameters to fit the normal flame velocity and the flame thickness, obtaining at least a qualitatively correct description of the flame dynamics. The situation is different for nonstationary processes, like ignition, transition processes, and the like. In a trivial way, taking e.g., an unrealistically high activation energy in order to match more or less accurately the induction time data from detailed chemistry, the parameters of the reduced one-step or two-step models can be chosen in order to reproduce the constant-volume induction time data or the homogeneous explosion. However, this choice of high activation energy leads to a totally incorrect ignition energy, and in addition the main reaction zone becomes exponentially thin, which considerably affects the velocity, thickness, dynamics, and stability of the flame.

Another difference is that for a one-step model the reaction is exothermic for all temperatures, while chain-branching reactions begin with a neutral or endothermic induction stage representing chain initiation and branching. Therefore, the gas dynamics is effectively “switched off” during the induction stage. The early phase of explosion determined by the spontaneous wave evolution is not affected by the gas dynamics. On the contrary, in the case of the one-step kinetics the mechanism of spontaneous wave propagation is considerably affected by the gas dynamics from the very beginning. Because of this the velocity of the spontaneous wave produced by the same temperature gradient in the early stage of the adiabatic explosion development when there is no gas-dynamic evolution is considerably different and smaller for the chain-branching reaction compared with that given by a one-step model. These differences between a one-step model and chain-branching chemistry significantly affect the ignition and evolution of spontaneous combustion wave, especially below the crossover temperature. Because of this all the regimes of combustion wave initiated by the temperature gradient occur for much shallower temperature gradients than those predicted by a one-step model.

Figures 1(a) and 1(b) show typical trajectories of the spontaneous and pressure waves initiated in a hydrogen-oxygen stoichiometric mixture by the temperature gradient for a single-step model [Fig. 1(a):  $T^* = 1500$  K,  $T_0 = 300$  K,  $L = 0.1$  cm] and for a detailed model [Fig. 1(b):  $T^* = 1500$  K,  $T_0 = 300$  K,  $L = 0.5$  cm]. For the steep (small  $L$ ) temperature

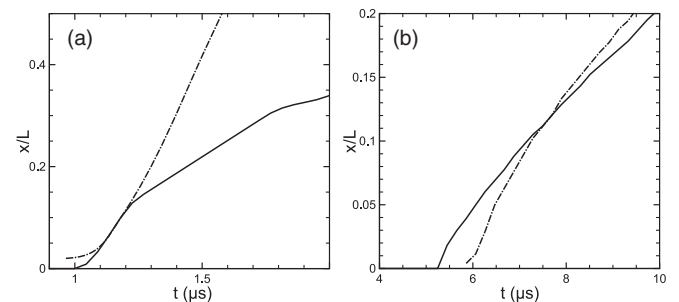


FIG. 1. Trajectories of the reaction wave (solid lines) and pressure wave (dash-dotted lines) for small values of  $U_{sp}$ : (a) a one-step model,  $T^* = 1500$  K,  $L = 0.1$  cm; (b) a detailed model,  $T^* = 1500$  K,  $L = 0.5$  cm.

gradient the pressure wave for the one-step model does not arise behind the spontaneous wave, as for the case of the detailed model, but from the very beginning it is formed ahead of the spontaneous wave. This feature of the single-step model remains similar for the shallower gradients. Therefore for a one-step model the gas dynamics always becomes the determining factor. As a result, the temperature gradient initiating all possible combustion regimes will be much steeper ( $L$  will be much smaller) for a single-step model compared to the gradient steepness calculated with detailed chemical kinetics.

#### IV. REGIMES OF CHEMICAL REACTION WAVE INITIATED BY THE TEMPERATURE GRADIENT IN $H_2-O_2$

In this section we investigate possible regimes of the combustion wave initiated by the temperature gradient with initial conditions given by Eqs. (2) and (3) for a hydrogen-oxygen stoichiometric mixture. In what follows we consider as the main variant temperature gradients of different steepness (different scale  $L$ ) at the initial pressure 1 atm with  $T^* = 1500$  K,  $T_0 = 300$  K unless otherwise specified. The calculated evolution of the reaction wave velocity (solid line) for a gradient of the scale  $L = 8$  cm in a  $H_2-O_2$  gaseous mixture is shown in Fig. 2 along with the pressure wave velocity (dash-dotted line). The velocity of the reaction spontaneous wave was determined from the trajectory of the reaction front position (position of the maximum H-radical isoline). The velocity of the pressure wave was determined from the trajectory of the maximum pressure point of the pressure wave profile. The velocity of the spontaneous wave initiated by the initial temperature gradient decreases while the wave propagates along the gradient, and reaches its minimum value at the point close to the crossover temperature where it is

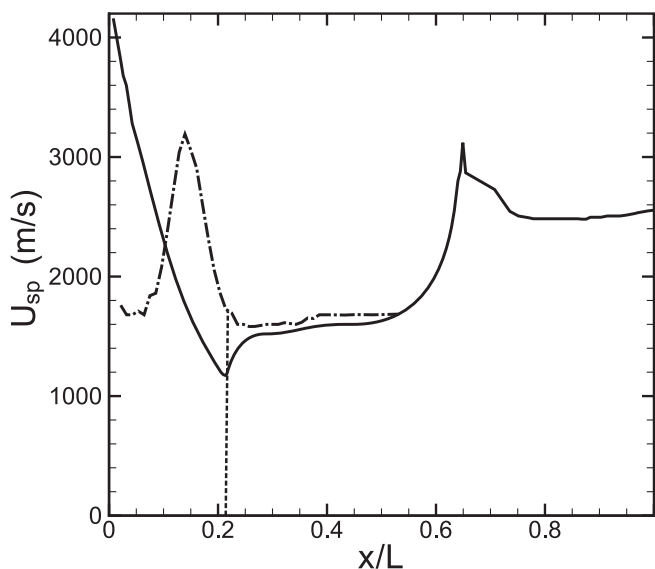


FIG. 2. Velocities of the spontaneous wave (solid line) and pressure wave (dash-dotted lines) computed for the temperature gradient  $L = 8$  cm,  $T^* = 1500$  K in a  $H_2-O_2$  mixture at the initial pressure  $P_0 = 1$  atm. The vertical dashed line shows the location of the maximum slowdown of the spontaneous wave, after which the pressure wave steepens into a shock wave.

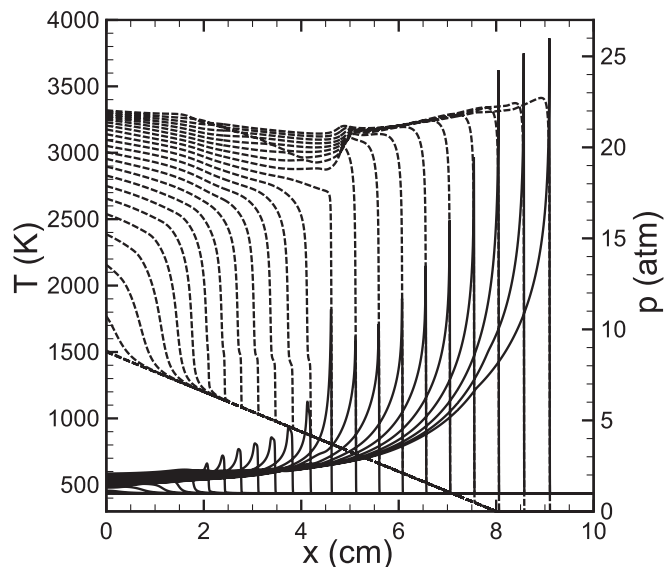


FIG. 3. Evolution of the temperature (dashed lines) and pressure (solid lines) profiles during the formation of the detonation in Fig. 2 shown at intervals of  $2 \mu s$ .

caught up with the pressure wave which was generated behind the high-speed spontaneous wave front. After the intersection of the spontaneous wave front and the pressure wave, the spontaneous wave transforms into a combustion wave and the pressure wave steepens into a shock wave. For a shallower gradient, such that the minimum speed of the spontaneous wave is of the order of the sound speed  $a_* = a(T^*)$  at the top of the gradient, the intensity of the shock wave formed ahead of the reaction wave is sufficient to accelerate the reaction wave in the flow formed behind the shock. As a result, a pressure peak is formed at the reaction front, which grows at the expense of energy released in the reaction. After the pressure peak becomes large enough, it steepens into a shock wave, forming an overdriven detonation wave (the peak of the maximum velocity  $U_{sp}$  at the point  $x/L = 0.65$  in Fig. 4). The evolution of the temperature and the pressure profiles corresponding to Fig. 2 is shown in Fig. 3.

If the initial temperature gradient is steeper (e.g., the gradient scale  $L = 7$  cm), then the velocity of the spontaneous wave at the minimum point, where the pressure wave overtakes the reaction wave, is not sufficient to sustain synchronous amplification of the pressure pulse in the flow behind the shock. As a result, the pressure wave runs ahead of the reaction wave as shown in Fig. 4 ( $L = 7$  cm), and the velocity of the reaction wave decreases. The corresponding temporal evolution of temperature and pressure profiles showing combustion wave formation behind the shock wave for the conditions of Fig. 4 is shown in Fig. 5.

The possible modes of the propagating combustion wave inspired by the spontaneous wave initiated by the temperature gradient depend on the gradient steepness. The pressure waves generated during the exothermic stage of reaction can couple and evolve into a self-sustained detonation wave, or produce a flame and a decoupled shock, depending on the gradient steepness. The outcome depends on the gradient steepness and the ratio between the speed of the spontaneous wave at the point

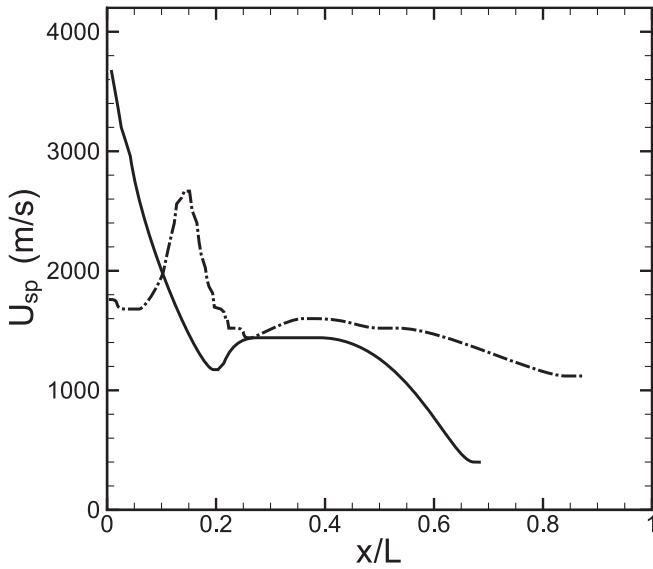


FIG. 4. Evolution of the spontaneous wave (solid curve) and pressure wave (dash-dotted line) velocities calculated for temperature gradient  $L = 7$  cm,  $T^* = 1500$  K in a  $\text{H}_2\text{-O}_2$  mixture, with  $P_0 = 1$  atm.

where its velocity reaches a minimum (minimum point) and the characteristic velocities of the problem:  $U_f$ ,  $a_0 = a(T_0)$ ,  $a^* = a(T^*)$ ,  $a_N$ ,  $a_{CJ}$ ,  $U_{CJ}$ . Here  $U_f$  is the normal laminar flame speed;  $a_0$ ,  $a^*$ ,  $a_N$ , and  $a_{CJ}$  are the speeds of sound at the points  $T = T_0$ , at  $T = T^*$ , at the Newman point, and at the Chapman-Jouguet point; and  $U_{CJ}$  is the velocity of Chapman-Jouguet detonation.

Possible combustion regimes obtained from the numerical studies with the detailed chemical kinetics depending on the gradient steepness and the speed of the spontaneous wave relative to the characteristic velocities of the problem are shown in Fig. 6, which represents the diagram for  $U_{sp}$  versus the inverse gradient steepness  $L = T/(dT/dx)$ . In summary, there are the following modes of reaction front propagation

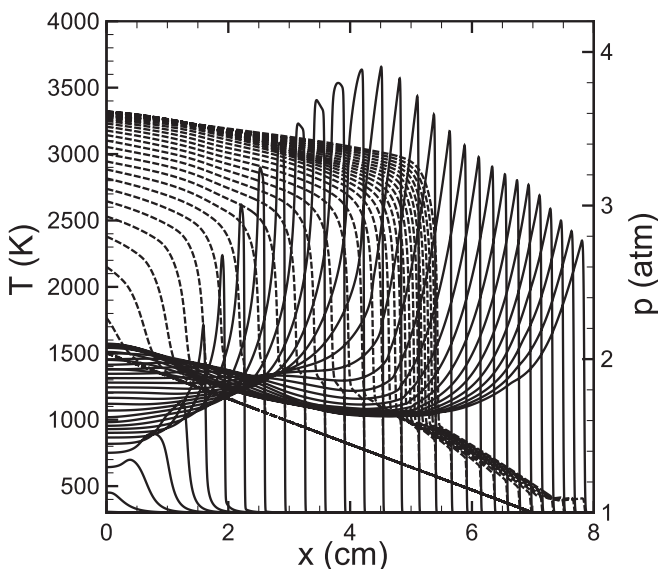


FIG. 5. Pressure (solid lines) and temperature (dashed lines) profiles evolution for the conditions of Fig. 4;  $\Delta t = 2 \mu\text{s}$ .

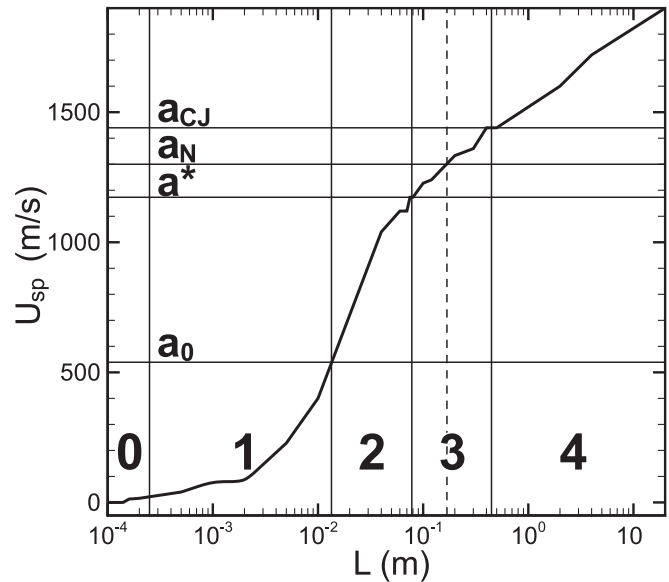


FIG. 6. Possible regimes of the reaction wave propagation initiated by temperature gradients of different steepness (different scales  $L$ ) in a  $\text{H}_2\text{-O}_2$  mixture, with  $P_0 = 1$  atm.

initiated by the initial temperature gradient. For  $U_{sp} < U_f \ll a_0$  (domain 0), the rate of the heat transfer by thermal conduction is greater than the spontaneous wave velocity, and the resulting regime is a deflagration wave propagating due to thermal conduction with the normal flame velocity  $U_f = 10$  m/s. Ignition of the deflagration is bounded from below by the minimum size of the hot region, for which the rate of heat removal from the “hot wall” is larger than the normal flame velocity. Domain (0) in Fig. 6 corresponds to the regime (4) in the Zeldovich classification [2]. If the spontaneous wave velocity at the minimum point is greater than the normal flame speed but less than the sound speed in the unperturbed medium,  $U_f < U_{sp} < a_0$  (domain 1), then “fast” deflagration occurs. The pressure wave overtakes the deflagration wave, and the fast deflagration wave propagates at nearly constant pressure. If  $a_0 < U_{sp} < a^*$ , then the pressure wave overtakes the reaction wave to form a weak shock wave that compresses and heats the gas, further speeding up the deflagration wave (domain 2). There are two different scenarios for domain 3, where  $a^* < \min\{U_{sp}\} < a_{CJ}$ . If  $a^* < \min\{U_{sp}\} < a_N < a_{CJ}$  the reaction wave accelerates behind the shock and a transition to detonation occurs due to the formation and amplification of the pressure peak at the front of the reaction wave. If  $a_N < \min\{U_{sp}\} < a_{CJ}$  then a quasistationary structure consisting of a shock wave and reaction zone is formed, which transforms into a detonation propagating down the temperature gradient. In both cases the spontaneous reaction wave is accelerated in the flow behind the shock wave and transits to a detonation wave. Both of these regimes correspond to a more detailed classification of regime 3 in the classification given in Ref. [2]. If  $a_{CJ} < \min\{U_{sp}\}$ , corresponding to the domain 4, then the intersection of the pressure wave and the spontaneous reaction wave creates a classical structure of a detonation wave with the leading shock wave initiating the reaction. Finally, the limiting case of very shallow temperature gradient  $\nabla T \rightarrow 0$ ,  $U_{sp} \rightarrow \infty$  corresponds to an adiabatic explosion.

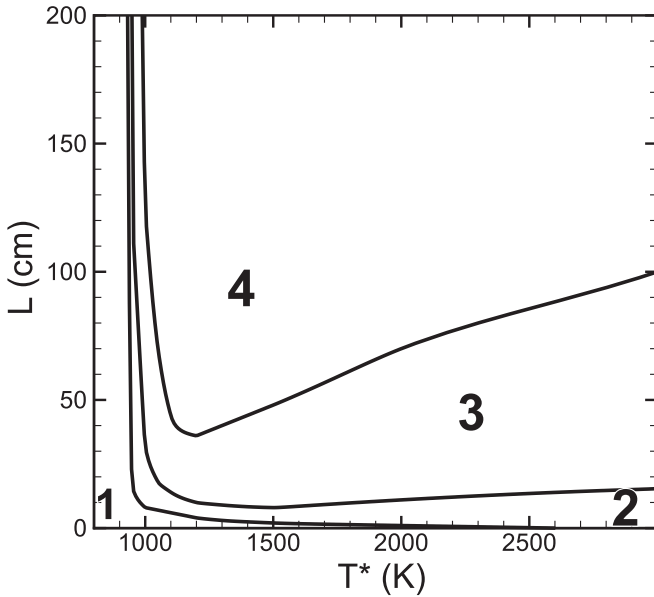


FIG. 7. Scales (inverse steepness) of the temperature gradient corresponding to the boundaries between regimes 1, 2, 3, and 4 in Fig. 6 calculated for a detailed chemical model depending on the value of  $T^*$ ;  $T_0 = 300$  K,  $P_0 = 1$  atm.

In summary, all the described regimes of the combustion wave initiated by the initial temperature gradient provide a more detailed classification of possible propagating combustion regimes disclosed first by Zeldovich [2] for a one-step chemical model.

### V. DEPENDENCE ON $T^*$

Figure 7 shows the limiting inverse gradient steepness corresponding to the boundaries between domains 1, 2, 3, and 4 in Fig. 6 versus temperature at the top of the gradient calculated for the detailed chemical model. The similar diagram in Fig. 8 for the boundaries between domains of the different modes calculated for the one-step chemical model shows us that at the initial pressure of 1 atm the steepness of the temperature gradient initiating any of the modes of the combustion wave is much shallower than that predicted by a one-step chemical model. This means that the size of the initial inhomogeneity initiating all the modes of combustion wave is much larger (10–20 times) than that predicted by a one-step chemical model. The gradient steepness and correspondingly its scale  $L = T/(dT/dx)$  capable of initiating one of the combustion regimes discussed above depends on the temperature at the top of the gradient. The marginal steepness between regimes 3 and 4 becomes maximal at  $T^* = 1200$  K and decreases with  $T^*$ . On the contrary, the domain of the “subsonic” modes (0 and 1) depends weakly on  $T^*$  since the mechanism of ignition of these regimes is similar to flame ignition by a hot wall. Besides the quantitative differences seen from Figs. 7 and 8, regime 3 corresponding to detonation initiation by the reaction wave accelerated in the flow behind the shock does not exist at high temperatures ( $T^* > 1500$  K) for a single-step model.

Since at lower temperatures the derivative  $d\tau_{\text{ind}}/dT$  is much larger than at high temperatures, the spontaneous wave

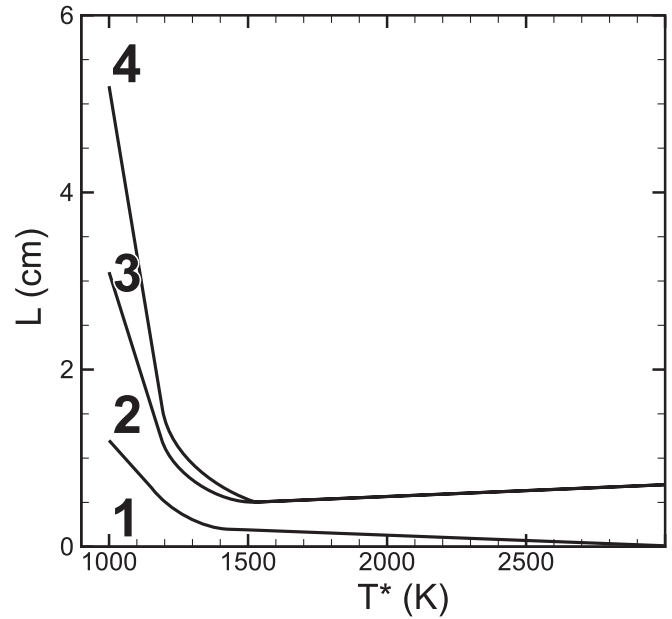


FIG. 8. Scales (inverse steepness) of the temperature gradient corresponding to the boundaries between different regimes calculated for a one-step model depending on the value of  $T^*$ ;  $T_0 = 300$  K,  $P_0 = 1$  atm.

velocity is smaller at low temperatures. Therefore at lower  $T^*$  initiation of the modes with a shock wave and detonation (modes 2, 3, and 4) requires much shallower gradients. At the same time  $d\tau_{\text{ind}}/dT$  is quite small at higher  $T^*$ , which results in larger initial velocity of the spontaneous wave. Slowing down of such fast spontaneous waves and the formation of shock or detonation waves require much shallower temperature gradients compared with the case of moderate  $T^*$ . This explains the increase of  $L = T/(dT/dx)$  for higher values of  $T^*$  in Fig. 7.

At higher temperatures the boundaries  $U_{1-2}$  and  $U_{2-3}$  between the modes 1 and 2 and 2 and 3 are almost independent of  $T^*$  because the induction time for  $T^* > 1500$  depends weakly on temperature. Also, since  $d\tau_{\text{ind}}/dT$  is small for  $T^* > 1500$  the realization of the modes with high velocity of the spontaneous wave initiating a detonation requires shallower gradients. It should be noted that, strictly speaking, the sound speeds at the upper and lower points of the temperature gradient give the scales defining the limits for different mode realizations only at a relatively high temperature  $T^*$  where the value of  $d\tau_{\text{ind}}/dT$  at the top of the gradient is not too large.

For lower values of  $T^*$  the regimes with initiation of shock and detonation waves require much shallower gradients. The corresponding scenario differs from the case with high temperatures  $T^*$  at the top of the gradient. As an example, Fig. 9 shows the velocities of the spontaneous wave (solid lines) and the pressure wave (dashed lines) for the formation of detonation (regime 3) for two temperature gradients:  $T^* = 1500$  K,  $L = 8$  cm (curves 1) and  $T^* = 1050$  K,  $L = 18$  cm (curves 2). At lower temperature  $T^* = 1050$  K the induction stage is about one order of magnitude longer than for  $T^* = 1500$  K. However, a more important qualitative difference is caused by the temperature value compared to the crossover

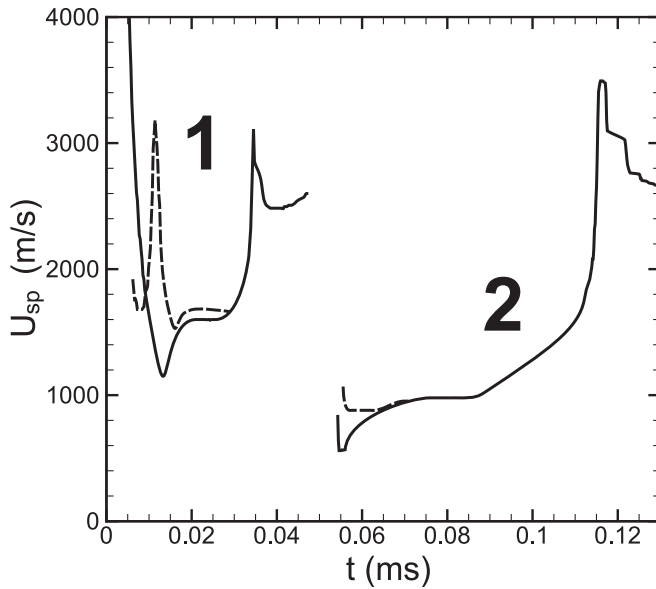


FIG. 9. The velocities of the reaction wave (solid lines) and pressure wave (dashed lines) corresponding to the formation of regime 3 in the temperature gradients = 1500 K;  $T_0 = 300$  K,  $L = 8$  cm (curves 1) and = 1050 K;  $T_0 = 300$  K,  $L = 18$  cm (curves 2).

temperature below which at lower temperature the induction stage becomes longer. Since in the region below the crossover temperature the induction stage is not fully endothermic, a small energy release during the long induction stage generates a pressure wave with a peak at  $x = 0$  before the reaction wave is formed. The pressure wave is formed immediately behind the reaction wave after the beginning of the termination stage. The pressure wave overtakes the subsonic exothermic reaction wave, creating a shock wave ahead of the reaction front. The intensity of the shock wave at lower values of  $T^*$  is determined by the velocity of the spontaneous wave directly at the point  $x = 0$ . On the contrary, for a one-step model a similar mechanism occurs for almost all temperatures, switching-on the gas dynamics from the very beginning of the process.

## VI. DEPENDENCE ON $T_0$

Of interest is the initiation of a combustion wave by a temperature gradient at relatively high ambient temperatures ( $T_0 \sim 1000$  K) outside the gradient. In this case the induction temperature range inside the gradient is beyond “the extended second explosion limit” (crossover), and for the same steepness of the gradient as for  $T_0 = 300$  K the reaction wave enters the high-temperature ( $T_0 \sim 1000$  K) region. However, in this case there is no hydrodynamic resistance outside the gradient since outside the gradient the wave propagates at constant ambient density, and therefore the transition to detonation may occur there for a steeper gradient (smaller  $L$ ). For steeper gradients the spontaneous wave velocity is lower, and the restructuring of the spontaneous reaction wave front in the flow behind the shock wave occurs after the wave leaves the temperature gradient, entering the region of ambient temperature. In this case, at later time in the induction stage, conditions for a local adiabatic explosion develop and a detonation wave arises

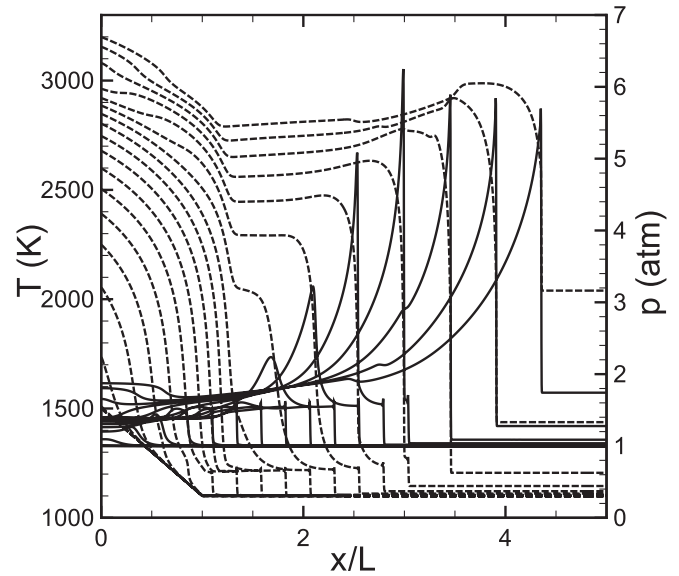


FIG. 10. Evolution of the temperature (dashed lines) and pressure (solid lines) profiles for the temperature gradient:  $T^* = 1500$  K,  $T_0 = 1100$  K,  $L = 1.0$  cm shown at intervals of  $2 \mu\text{s}$ .

behind the shock wave. Such regimes in a hydrogen-oxygen mixture were examined in Ref. [16], where ignition in closed spaces with high ambient temperature greater than or about 1000 K was investigated.

In fact, the induction stage which is distinctive for chain reactions is “skipped” at sufficiently high ambient temperatures, and the scenario of the detonation wave formation outside the gradient becomes more similar to what occurs for a single-step model. It should be noted that such a scenario of detonation formation outside the gradient is almost always present for a single-step model when a shock wave is formed. Above we did not consider these regimes since the detonation initiation within the gradient domain is of the main interest. Due to the high ambient temperature outside the gradient a volume explosion may occur since the arrival time of the reaction front may be less than the induction period. Since the velocity of the spontaneous waves is significantly lower, a thermal explosion may occur before a detonation wave is formed.

Figure 10 shows the evolution of temperature and pressure profiles illustrating the process described above. Once formed inside the gradient domain the shock wave leaves the gradient at  $x/L = 1.1$ . A new spontaneous reaction wave appears behind the shock at  $x = 1.4L$  directly in front of the combustion wave (at the point of maximum reactivity and minimal induction time), propagating along the gradient of reactivity formed behind the shock wave and initiating a detonation wave at  $x = 3.0L$ . However, at this time a mixture ahead of the shock wave has already passed the induction stage, and a volume explosion occurs ahead of the detonation wave. As a result the detonation wave becomes a shock propagating in the bulk of the explosion products.

For steeper gradients the intensity of the shock wave may not be enough for a local explosion to occur during the induction time in the mixture behind the shock. In this case the volume explosion ahead of the shock occurs before a detonation can be formed. Note that spontaneous ignition

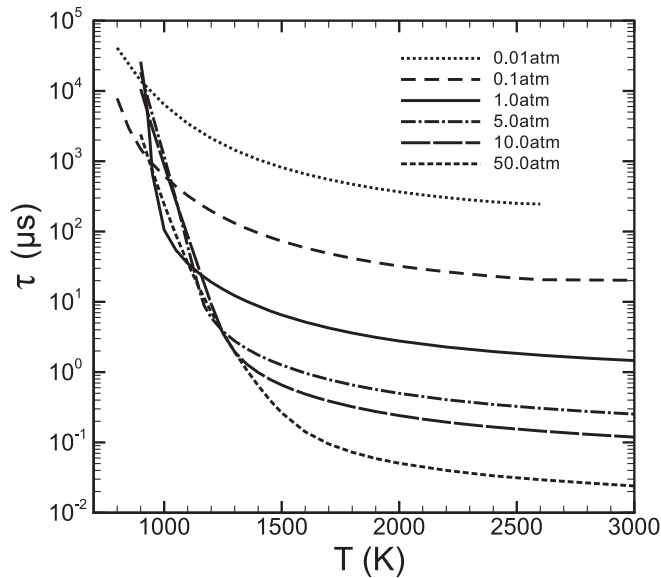


FIG. 11. Induction time versus temperature for hydrogen-oxygen mixture at different pressures 0.01–50 atm.

of the reaction behind the detached shock also describes the process of ignition in shock tube experiments, where a reflected shock of sufficiently high intensity propagates through a precompressed and preheated mixture at different stages of the induction phase. An additional heating of the mixture by the shock wave creates the conditions for the spontaneous ignition of the reaction behind it.

## VII. THE PRESSURE DEPENDENCE

The temperature dependence of the induction time changes when the initial pressure is changed. At lower pressures, the induction zone is much longer than the chain termination exothermic zone. At high pressures, when triple collisions dominate, they become of the same order (Fig. 11). The crossover temperature at which the equilibrium of the induction and termination stages takes place is known as the extended second explosion limit [27]. At higher pressures this limit shifts to higher temperatures and correspondingly at lower pressures it shifts to lower temperatures. Therefore, the initiation process at low pressures is qualitatively similar to the initiation of combustion waves at normal pressure for high temperature  $T^*$ . In this case the steepness of the temperature gradient required to implement the regimes with shock and detonation waves decreases rapidly, and the “speed” limits separating regions of different modes are determined by the sound speeds  $a_0$ ,  $a^*$ , and  $a_C$ . On the contrary, in the case of high pressure the scenario is somewhat more similar to that realized for a one-step model or for low values of  $T^*$ , resulting in a decrease in the limits of ranges for the realization of regimes 2 and 3. At the same time, since at high pressure the induction time is considerably smaller, the minimal steepness of the gradients necessary for the implementation of all the regimes and in particular for the direct initiation of detonation is significantly increased (the minimal  $L$  decreases).

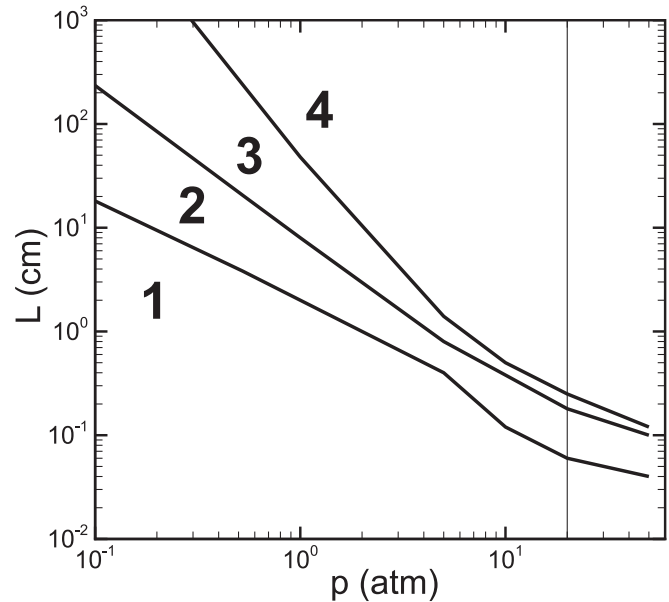


FIG. 12. Scales of the temperature gradient required for initiation of the regimes 1, 2, 3, and 4 depending on the initial pressure of  $H_2-O_2$  mixture ( $T^* = 1500$  K,  $T_0 = 300$  K).

Figure 12 shows how the inverse steepness (the gradient scale) of the temperature gradients changes depending on the initial pressure for the regimes 1, 2, 3, and 4, where the scales of the gradient were calculated for  $T^* = 1500$  K and  $T_0 = 300$  K. At lower pressure the regions of implementation of the slow-combustion regimes (1 and 2) become larger while regimes with the initiation of a detonation require much shallower gradients to produce fast enough spontaneous waves and the necessary conditions for its slowing down. With increasing pressure above 5 atm the region for the implementation of regime 2 slightly increases. At pressure 5 atm the length of the induction stage is about the length of the chain termination stage at  $T \sim 1200$  K. Therefore, part of the gradient with  $T^* = 1500$  K, where detonation can occur behind the shock wave (mode 3), decreases and a shallower gradient is needed for the implementation of mode 3. At pressures above 10 atm and for  $T^* = 1500$  K, the time of the induction phase exceeds the time of the exothermic reactions. Therefore, all combustion regimes are formed at high pressure, similarly to the scenario at low  $T^*$ , which is defined by the speed of the spontaneous wave at  $x = 0$ . At sufficiently high pressures (of the order of 50 atm), direct initiation of detonation by the temperature gradient in a hot spot of size 3–5 mm becomes possible. Direct initiation of detonation by the temperature gradient in a hot spot at a pressure of about 70 atm as the mechanism explaining the knock occurrence in engines was studied in Ref. [28] with a detailed chemical model.

## VIII. REACTION WAVE INITIATED BY THE TEMPERATURE GRADIENT IN HYDROGEN-AIR MIXTURES

The induction time increases if a combustible mixture is diluted by a neutral gas and for less reactive mixtures. For

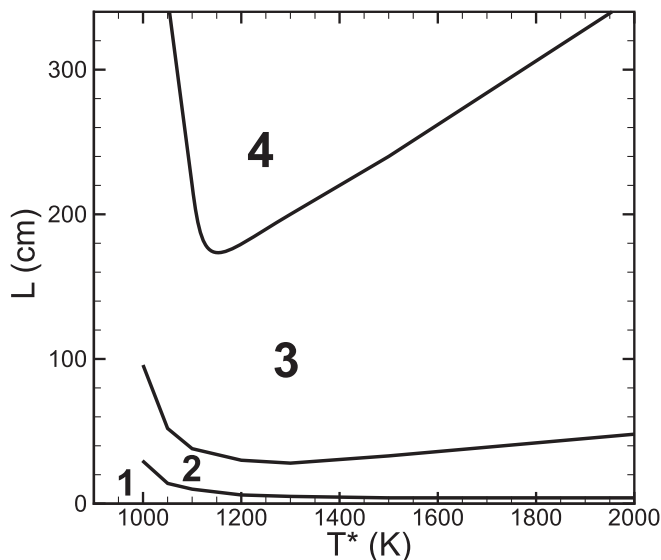


FIG. 13. Scales of the temperature gradient in a  $\text{H}_2$ -air mixture required for initiation of the regimes 1, 2, 3, and 4 depending on the  $T^*$  value;  $T_0 = 300$  K,  $P_0 = 1$  atm.

example, in a stoichiometric hydrogen-air mixture, which can be viewed as  $\text{H}_2$ - $\text{O}_2$  diluted by nitrogen not involved in the chain-branching reaction, the induction time increases by 2–3 times in a wide temperature range compared to a stoichiometric hydrogen-oxygen mixture. At the same time the main features of the induction time dependence versus temperature and pressure remain nearly the same. So the main difference between hydrogen-air and hydrogen-oxygen mixtures is the reduced velocity of spontaneous waves for the same temperature gradients. As a result, the temperature gradient required for realization of various combustion regimes in the hydrogen-air mixture is significantly shallower than in the hydrogen-oxygen mixture. This is illustrated in Fig. 13 which shows the temperature gradient scales depending on  $T^*$  calculated for the detailed chemical model for a  $\text{H}_2$ -air mixture, and depicting the domains of gradient steepness required for initiation of the regimes 1, 2, 3, and 4 at initial pressure  $P_0 = 1$  atm.

Above it was shown that the limits of formation of different combustion regimes also depend on the characteristic velocities in the problem. The sound speed in a hydrogen-air mixture is about 25%–30% smaller than in the hydrogen-oxygen mixture. The difference in magnitude is maximal for  $a_{CJ}$  and minimal for  $a_0$ . Since the characteristic scale of the velocity for regime 4 is the sound speed at the Chapman-Jouguet point, the length of the gradient required for the formation of regime 4 in a hydrogen-air mixture increases more significantly. The lower limit for regime 2 is the sound speed  $a_0$ . Correspondingly, the length of the gradient for regime 2 in a hydrogen-air mixture increases by approximately two times compared to the hydrogen-oxygen mixture.

The reduced reactivity of a hydrogen-air mixture compared to hydrogen-oxygen in the example above is due to the lower concentration of the reacting molecules diluted by nitrogen molecules. The peculiarities of the chemical kinetics for other slowly reacting mixtures, such as hydrocarbon-oxygen

mixtures, may be qualitatively different. For example, the induction time versus temperature and pressure in methane-oxygen and ethane-oxygen mixtures is a monotone function, and the reaction mechanism does not change with temperature and pressure. The kinetic model for iso-octane and *n*-heptane includes cool flames so that the exothermic reaction can start at low temperatures during the induction phase. This model was used in Refs. [23,24] to explain the formation of hot spots and knock occurrence in engines.

## IX. CONCLUSIONS

In the present paper we used detailed chemical kinetics models to study the combustion regimes in stoichiometric hydrogen-oxygen and hydrogen-air mixtures ignited by the initial temperature gradient. The problem in question was studied using high-resolution numerical simulations, and the results obtained give the scales of the initial temperature nonuniformity and the amount of energy required for ignition of one or another regime of combustion. It was shown that the evolution of a spontaneous wave from the initial temperature gradient is significantly quantitatively different and may be even qualitatively different for the chain-branching kinetic model compared with the predictions from a one-step model. As a consequence, combustion regimes initiated by the temperature gradient require much shallower (up to several orders of magnitude) gradients compared with those predicted by a single-step model. The difference between a one-step model and a detailed chemical model is especially noticeable at lower pressures and for slowly reacting mixtures. For example, the steepness of the temperature gradient for direct initiation of detonation in a hydrogen-air mixture is more than 100 times smaller than is predicted by a one-step model. One of the conclusions is that, contrary to what has been thought previously, the mechanism of transition from deflagration to detonation cannot be a temperature gradient within hot spots, since the size of a hot spot is too small and the scales corresponding to the steepest temperature gradient required for the direct initiation of detonation are too large compared to the size of the hot spot for any practical fuels. To initiate a detonation, the temperature gradient must be shallow enough to build a strong pressure peak, which is of the magnitude of the von Neumann pressure peak in a detonation wave. It was shown that for high pressures the gradient steepness for direct initiation of detonation decreases considerably, which means that at very high pressure the detonation can be ignited by a small-scale initial nonuniformity, which is of substantial practical interest for *risk assessment* to minimize accidental explosions, in particular, for safety guidelines in industry and nuclear power plants.

The critical steepness of the temperature gradients separating the regimes of strong and weak coupling between pressure and the spontaneous wave depends on the initial pressure and reactivity of the combustible mixture. At very high initial pressures ( $>50$  atm), direct initiation of detonation becomes possible from an initial temperature nonuniformity of the order of a few millimeters. For high enough ambient temperatures ( $T_0 \geq 1000$  K) the detonation can be formed outside the gradient in  $\text{H}_2$ - $\text{O}_2$  mixtures. Furthermore in the case of high ambient temperatures a temperature gradient capable

of producing a spontaneous wave igniting a detonation can be formed due to the compression and heating behind the shock. Thus, the results obtained. Thus, the obtained results answer the question important for practical applications: what are the ignition energy and the scales of energy deposition (e.g., the scale of the nonuniformity produced by the igniter) capable of igniting one or another regime of propagating combustion wave. It should be noted that in investigations of the chemical reaction kinetics using experimental techniques utilizing shock tubes, rapid compression machines, flow reactors, etc., the gas dynamics always significantly influences the ignition. On the contrary, the problem of combustion waves initiated by a given temperature gradient opens additional avenues to reveal features of the chemical kinetics in cases when the evolution of the spontaneous reaction wave is defined solely by the kinetics of the combustion. The results of this work may be the basis for further experimental techniques, based on the creation of a temperature gradient without strong initial hydrodynamic perturbations.

#### ACKNOWLEDGMENTS

The paper has benefited greatly from discussions with N. Popov. Comments by A. Kapila are also acknowledged.

#### APPENDIX: CODE VALIDATION: THE CONVERGENCE AND RESOLUTION TESTS

Resolution and convergence tests were thoroughly performed to ensure that the resolution is adequate to describe and to capture details of the problem in question and to avoid computational artifacts. This is especially important for a mixture consisting of many species with a large number of reactions in the case of a detailed chemical model, when application of analytical methods is limited. The convergence and resolution tests for a planar laminar flame front [21,22] have shown that convergence of the solution is quite satisfactory even for eight computational cells per flame width, when the flame width, the flame velocity, density, and temperature differ by less than 2% from the converged solution, while a resolution of 16 computational cells results in an exact solution. For a combustion wave initiated by a linear temperature gradient the main parameter is the steepness of the gradient [its scale  $L = T/(dT/dx)$ ] corresponding to the transition between regimes 2 and 3 for the given initial conditions  $T^*, T_0, P_0$ . At  $P_0 = 1$  atm an exact solution for a laminar flame occurs for a resolution of 50 cells over the flame width, which corresponds to the size of the cell 0.0064 mm, as shown in Figs. 14 and 15. According to the flame width dependence on pressure, the resolution and the size of the computational cell were increased or decreased for higher or lower pressures. It should be noted that during the spontaneous wave propagation stage a high resolution is not critical for the evolution of the reaction and the pressure waves smoothly spread over the space. However, a proper resolution is important after the pressure wave steepens into a shock since the computational scheme spreads the shock front over five cells for stable modeling of a discontinuity. This concerns, for example, modeling of regime 3, where the mechanisms of detonation formation are qualitatively different depending on the relation between

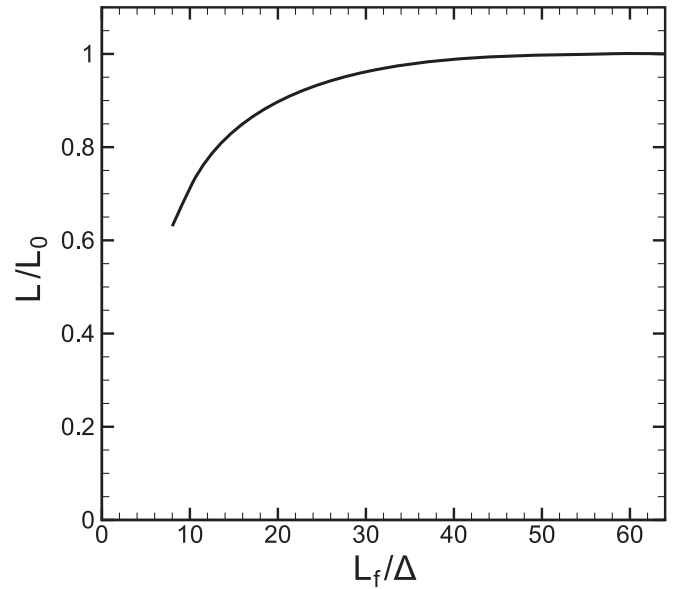


FIG. 14. Scales of the temperature gradients for the boundary between regimes 2 and 3 calculated with different resolutions, illustrating convergence of the solution.

$\min\{U_{sp}\}$  and  $a_N$ . A finite smearing of the shock front in this case may affect the formation and growth of the pressure peak at the front of the reaction wave and correspondingly distort the formation of the detonation wave according to the scenario of regime 3 for  $\min\{U_{sp}\} < a_N$ . Figure 15 shows that convergence of the solution is quite satisfactory according to this for 16 computational cells per flame width, which coincides with the resolution for the converged solution of a laminar flame [21,22].

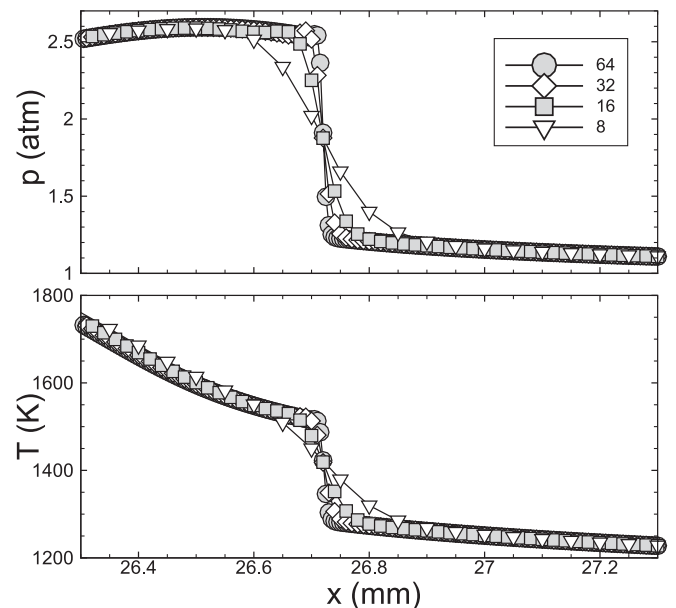


FIG. 15. The pressure profile in a shock wave formed at  $17.5 \mu\text{s}$  due to spontaneous wave propagation in the temperature gradient  $T^* = 1500$  K,  $T_0 = 300$  K,  $L = 10$  cm calculated with resolutions 8, 16, 32, and 64 cells over the flame width.

- [1] T. Echekki and J. H. Chen, *Combust. Flame* **134**, 169 (2003).
- [2] Ya. B. Zeldovich, *Combust. Flame* **39**, 219 (1980).
- [3] Ya. B. Zeldovich, V. B. Librovich, G. M. Makhviladze, and G. I. Sivashinsky, *Astronaut. Acta* **15**, 313 (1970).
- [4] B. E. Gelfand, A. N. Polenov, S. M. Frolov *et al.*, *Fiz. Gorenia Vzryva* **4**, 118 (1985).
- [5] B. E. Gelfand, S. M. Frolov, A. N. Polenov *et al.*, *Chem. Phys.* **9**, 1277 (1986).
- [6] Ya. B. Zeldovich, B. E. Gelfand, and S. A. Tsyganov, *Prog. Astronaut. Aeronaut.* **14**, 99 (1988).
- [7] G. Singh and J. F. Clarke, *Proc. R. Soc. London, Ser. A* **438**, 23 (1992).
- [8] N. Nikiforakis and J. F. Clarke, *Math. Comput. Modell.* **24**, 149 (1996).
- [9] L. He, *Combust. Flame* **104**, 401 (1996).
- [10] A. K. Kapila *et al.*, *Combust. Theory Modell.* **6**, 553 (2002).
- [11] J. W. Dold and A. K. Kapila, *Combust. Flame* **85**, 185 (1991).
- [12] G. J. Sharpe and M. Short, *J. Fluid Mech.* **476**, 267 (2003).
- [13] Z. Liang and L. Bauwens, *Combust. Theory Modell.* **9**, 93 (2005).
- [14] G. J. Sharpe and N. Maflahi, *J. Fluid Mech.* **566**, 163 (2006).
- [15] T. M. Sloane and P. D. Ronney, *Combust. Sci. Technol.* **88**, 1 (1992).
- [16] H. J. Weber and A. Mack, P. Roth, *Combust. Flame* **97**, 281 (1994).
- [17] J. Warnatz, U. Maas, and R. W. Dibble, *Combustion. Physical and Chemical Fundamentals, Modeling and Simulations, Experiments, Pollutant Formation* (Springer, Berlin, 2001).
- [18] J. B. Heywood, *Internal Combustion Engine Fundamentals* (McGraw-Hill, New York, 1988).
- [19] J. O. Hirschfelder, C. F. Gurtiss, and R. B. Bird, *Molecular Theory of Gases and Liquids* (Wiley, New York, 1964).
- [20] O. M. Belotserkovsky and Yu. M. Davydov, *Coarse-Particle Method in Hydrodynamics* (Nauka/Mir, Moscow, 1982).
- [21] M. F. Ivanov, A. D. Kiverin, and M. A. Liberman, *Phys. Rev. E* **83**, 056313/1 (2011).
- [22] M. F. Ivanov, A. D. Kiverin, and M. A. Liberman, *Int. J. Hydrogen Energy* **36**, 7714 (2011).
- [23] M. A. Liberman, M. F. Ivanov, and D. M. Valiev, *Combust. Sci. Technol.* **178**, 1613 (2006).
- [24] M. A. Liberman, M. F. Ivanov, O. D. Peil, and D. M. Valiev, *Combust. Sci. Technol.* **177**, 151 (2005).
- [25] D. Lewis and G. von Elbe, *Combustion, Flames and Explosion of Gases*, 2nd ed. (Academic Press, New York, 1961), Part 1.
- [26] Ya. B. Zeldovich, G. I. Barenblatt, V. B. Librovich, and G. M. Makhviladze, *The Mathematical Theory of Combustion and Explosion* (Plenum, New York, 1985).
- [27] B. E. Gelfand, O. E. Popov, B. B. Chivanov, *Hydrogen: Parameters of Combustion and Explosion*, Fizmatlit, Moscow 2008 (in Russian); see also E. Schultz and J. Shepherd, *Validation of Detailed Reaction Mechanisms for Detonation Simulation*, Cal. Inst. of Tech. Graduate Aeronautical Lab. Tech. Rep. FM 99-5 (2000), p. 230.
- [28] X. J. Gu, D. R. Emerson, and D. Bradley, *Combust. Flame* **133**, 63 (2003).